Experimental investigation of cyclically sheared granular particles with direct particle tracking

Andreea Panaitescu and Arshad Kudrolli*)

Department of Physics, Clark University, Worcester, MA 01610, U.S.A.

(Received November 29, 2009)

We discuss experiments on dense packing of granular beads that are cyclically sheared quasi-statically between parallel walls under constant pressure boundary conditions. The particle positions inside the shear cell are tracked over several cycles in three dimensions using particle index-matching imaging technique. The total volume fraction of the particles ϕ in the cell is observed to increase slowly over thousands of cycles from $\phi \sim 0.59$ to $\phi \sim 0.63$, while even slower growth in volume fraction is observed in the bulk away from boundaries. We illustrate with internal images that the difference arises due to inhomogeneity of packing with ordered regions developing progressively from the boundaries. We then focus in the bulk where the packing is uniformly disordered, and find that a linear bulk strain is observed within the first half of a cycle, which is reversed in the second half of the cycle. We present analysis of the trajectories of the particles within a shear cycle as well as over several cycles. We find anisotropic fluctuations relative to shear gradient within a cycle. However, homogeneous growth of mean square displacement when fluctuations are examined average over a cycle. The rate of growth is significantly lower leading us to hypothesize that granular matter under cyclic shear show reversible as well as irreversible or plastic response for small enough strain amplitude.

§1. Introduction

The response of inelastic hard spheres to applied shear is arguably one of the most important questions in non-equilibrium physics and fundamental to describing granular flows. Because of the dissipative nature of particle-particle interactions and the athermal nature of the system, particles quickly come to rest unless energy is input into the system. Further, when external energy is supplied, it remains unclear if particles explore all phase space as in thermal systems or get trapped in a local attractor - which is typical of dissipative systems. While progress has been made using kinetic theory approaches in the low volume fraction regime,[1)–3)] it is far from clear that such an approach can be applied at higher volume fraction and especially where enduring contacts occur between particles as system begins to jam.

One measure of the response in a sheared particle flow is the self-diffusion of particles measured from the non-affine mean square displacement of the particles. Campbell[4)] first reported with computer simulation that self-diffusion was anisotropic, but system size was an important factor. Later, Foss and Brady[5)] performed larger scale Brownian dynamics simulations for particles without hydrodynamic interactions, and showed that the measured diffusion constant measured along the flow direction is greater than in the gradient direction which in turn is greater than in the vorticity direction. More recently, Kumaran[6)] has concluded that sheared

*) Corresponding Author E-mail: akudrolli@clarku.edu

granular packings remain in the disordered state at volume fractions ϕ above 0.49 where elastic spheres would order, and dynamics is determined by volume fraction and coefficient of restitution.

Particle diffusion properties have been measured in granular shear experiments, but these results have been confined to either two dimensional systems[7] or three dimensional systems[8),9] where the shear occurs near a boundary which induces layering and thus boundary effects could not be decoupled. While such studies have added valuable insight, it is important to examine properties directly in the bulk in three dimensions to ascertain their properties. Therefore, there is a great need for an experiment which examines sheared granular dynamics away from the side walls with three dimensional particle tracking.

In this paper, we discuss experiments with spherical glass particles subjected to quasi-static cyclic shear where we obtain bulk shear within a cycle and where we track the three dimensional position of the particles using an index matched interstitial liquid. Our system is similar to a cyclic shear system used by Pouliquen, *et al.*[11] to study caging of tracer particles. However, our system has a lower height to width cell aspect ratio which allows a nearly linear shear strain in the region of interest within a shear cycle. Further, using a laser sweeping technique, we can track all the particles in full 3-D in the region of interest to directly determine local volume fraction and packing structure, and link it to particle rearrangements. From the measured particle positions, we obtain the evolution of the packing fraction, probability distributions of particle displacements, and mean-squared displacements relative to applied shear gradient. Using these measurements we discuss anisotropy of the diffusion, and the reversible and plastic response of the system.

Our experiments build on work performed by our group on self-diffusion in gravity driven flows sheared by a side wall. These experiments have shown a slow decay of the velocity auto-correlation function (VACF) for unsheared granular flows[10] consistent with hard sphere simulations of dense liquids and fast decay of velocity auto-correlation functions[9] consistent with recent theoretical work[12),13] on linearly sheared inelastic particles, although the exponent could not be confirmed. While these experiments image particles in an illuminated plane inside a three dimensional flow, the new experiments reported here use three dimensional tracking of particles rather like confocal microscopy technique used to study oscillatory shear by Toiya, *et al*[14] but here using a more rudimentary technique which allows us to look into greater depth inside the packing.

A natural issue in such experiments is the impact of the interstitial liquid used to enable visualization on granular fluctuations. In other words, can drag and lubrication forces be considered small enough in these experiments, just as interstitial air is considered negligible in typical dry granular systems. While, drag forces are easily estimated, the lubrication forces are harder to predict because particle roughness and relative velocity is difficult to estimate to sufficient precision. Over the last few years, work done by our group has shown that at sufficiently slow flow and shear rates, the interstitial liquid play no discernible role in measured shear forces and particle rearrangements for millimeter size grains, and compare well to those in dry granular flow, where such measurements can be made. First, by measuring the shear

force experienced by a sliding wall on a granular surface,[16] it was shown that for sufficiently slow strain rates, the frictional drag experienced is within experimental error of 1% of the dry case. Second, we were able to obtain excellent agreement by performing direct comparisons of particle rearrangements with molecular dynamics simulations which completely neglects the interstitial fluid.[17] In our current experiments, the flow is imposed quasi-statically, and the confining pressure is 10 times greater than in the experiments reported in Ref. 16). Therefore, we claim that particles are in enduring contact as the system is sheared, and the interstitial fluid is not important to the observed fluctuations.

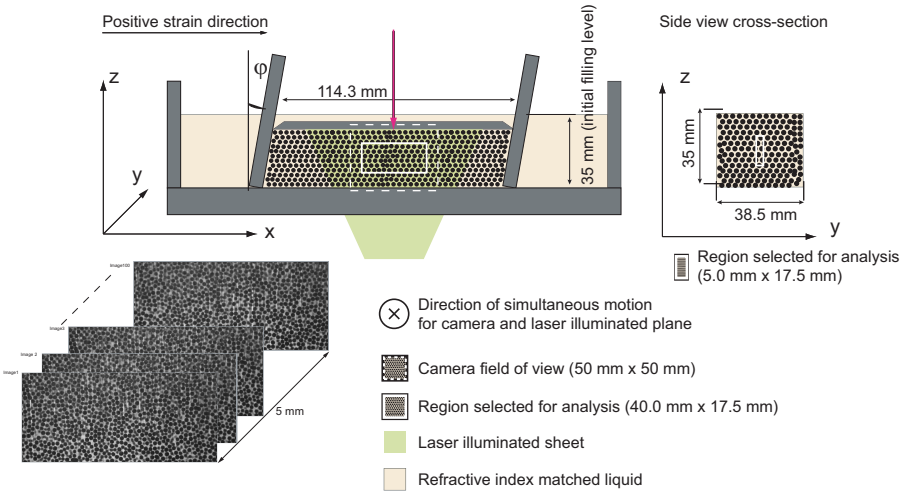

Fig. 1. (Color online) A schematic diagram of the granular cyclic shear cell apparatus. The vertical walls of the shear are rotated between $\theta_0 = -\pi/36$ radians, and $\theta_0 = \pi/36$ radians in 30 equal steps. The same shear is then applied in the opposite direction to complete a cycle, and the cycle is repeated over 2000 times while recording a stack of images to track particle positions. A constant normal stress of 0.4 Pa is applied at the top boundary, but is otherwise free to slide vertically to allow any change in volume fraction in response to applied shear.

§2. Experimental Apparatus

2.1. *The shear cell*

A schematic diagram of our experimental apparatus is shown in Fig. 1. Uniform glass beads with diameter $d = 1.034 \pm 0.024$ mm, are placed inside a rectangular box with transparent smooth glass side walls. The front, back and bottom walls are rigidly attached. The top boundary is constrained to move only in the vertical and horizontal direction and not allowed to rotate using a rigid set of linear guides. A fixed normal stress $\sigma_n = 0.4$ Pa is applied on the top boundary which is about five times the gravitational stress due to the weight of the grains alone inside the box, to decrease any effect of gravitational gradient. The side walls, which are attached

with hinges to the bottom boundary, can be tilted from the vertical through a given angle θ with a stepper motor and gear system, thus applying shear strain to the system. In the experiments reported here, θ was incremented between $-\theta_0$ and θ_0, where $\theta_0 = \pi/36$ radians in $\Delta\theta_0 = \theta_0/15$ increments. Then the applied strain was reversed and the vertical wall was returned to $-\theta_0$ using the same protocol. This applied shear cycle was then repeated more than 2150 times.

2.2. *Imaging technique*

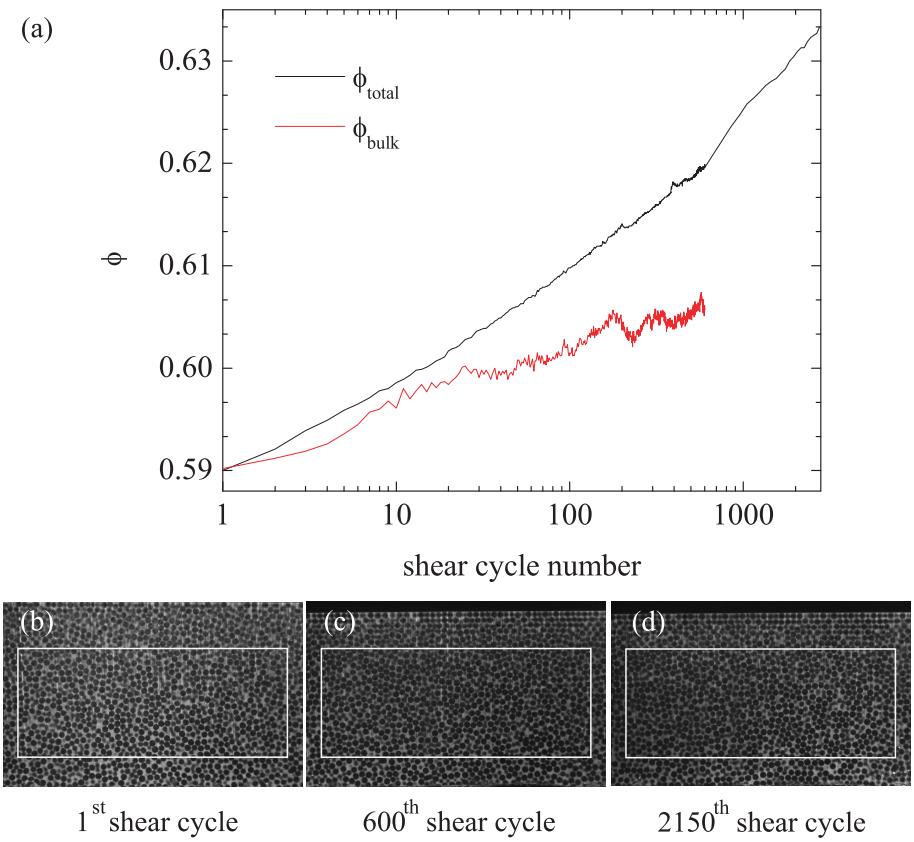

Fig. 2. (Color online) (a) The total volume fraction of the grains inside the shear cell as a function of shear cycle number N measured using the height of the top boundary, and the volume fraction measured in the bulk by counting the number of particles inside the viewing region. The differences arise because spatial inhomogeneity in the packing in different parts of the cell. Sample images for (b) $N = 1$,(c) $N = 600$, and (d) $N = 2150$ shows that hexagonal ordering first occurs at the top near the moving boundary and progresses downward into the cell.

To visualize the grains, an index matched liquid is added along with a fluorescent dye which is illuminated with a laser sheet similar to that used in our previous experiments.[10),16)] Because the strain is applied quasi-statically, we sweep the laser which is mounted on a linear translating stage (not shown) along with a 1024×1024 pixel digital camera after each strain step[14)] in the y-direction, to obtain a stack of images examining different image planes inside the cell in steps of $50\,\mu$m. No

significant relaxation of particles is observed if the wait time between obtaining a scan is varied from within a second to minutes. However, slow relaxation is observed if the system is left under compression over night as has been also noted previously.[18] As illustrated in Fig. 1, we focus in a $5d$ deep section in the center of the shear cell to minimize the effect of side walls in the analysis that we present here. We find dark voxels corresponding to the sphere in a bright background using standard imaging algorithms based in IDL computing environment,[19] and locate the absolute center of the glass bead using a sub-pixel centroid algorithm to within the $0.05d$ sphericity of the particles, and relative changes in its position to well within 1%.

In Fig. 2, the average packing fraction ϕ of the glass beads observed inside the shear cell is plotted as a function shear cycle using two techniques. First, we measure the height of the top boundary, and thus obtain the average volume fraction of the spheres. The packing fraction is observed to increase rapidly first from $\phi = 0.59$ of the initial packing obtained by pouring, and then more slowly to over $\phi = 0.63$ as was also reported previously.[11] However, it is important to note that measuring the volume fraction using this method assumes the packing to be uniform inside the cell. To illustrate this is not the case, we show images of the center vertical cross-section of the cell after cycle number $N = 1$, $N = 600$, and $N = 2150$. Crystalline packing starts to appear at the top boundary and progresses further down as N is increased. In Fig. 2, we also plot the volume fraction away from the side walls of the container by counting the number of particles inside the central $40d \times 5d \times 17.5d$ region of the cell indicated by the box in Fig. 2 and in Fig. 1. Only data in the range $N < 601$ is shown because high quality images were obtained in this data range where we could identify all the particles in the viewing window. Clearly, the volume fraction increases but much more slowly. Further, we can note that the structure of the packing appears rather disordered in the bulk as seen from the images of the particles for these volume fractions of $\phi \sim 0.61$ after application of cyclic shear. This is an essential difference from sheared elastic spheres at similar high densities.[6] Because here we are interested in the diffusion in an uniformly random system, we focus in the bulk regions where no visible order is present for $N \lessapprox 600$.

§3. Experimental Data

3.1. *Strain profile*

The applied strain is small enough so that we can track the position of the grains between consecutive steps and over many cycles, provided the grains stay within the viewing window illustrated in Fig. 1. From these tracks, we have obtained the individual displacement of the particles. In Fig. 3, we plot a set of particle displacements corresponding to rotating the side walls by a small angle in the flow $-x$, vorticity $-y$, and gradient $-z$ directions. Individual points corresponds to 5×10^4 measurements obtained over a single strain step at various heights inside the cell. While the particle displacements are centered around zero for y, and z directions, the displacements clearly grow with height inside the cell from the stationary boundary at the bottom to the moving boundary at the top. Further by obtaining the mean

displacement as a function of height - denoted by red large points in Fig. 3(a) - it is also clear that we have succeeded in producing a broadly sheared system away from the boundaries. By fitting the observed mean displacements, we find that the particles are strained linearly to within 1% over $20d$, and the corresponding strain gradient in z-direction $\gamma_z = 2.4 \times 10^{-1}$ per unit radian of applied strain.

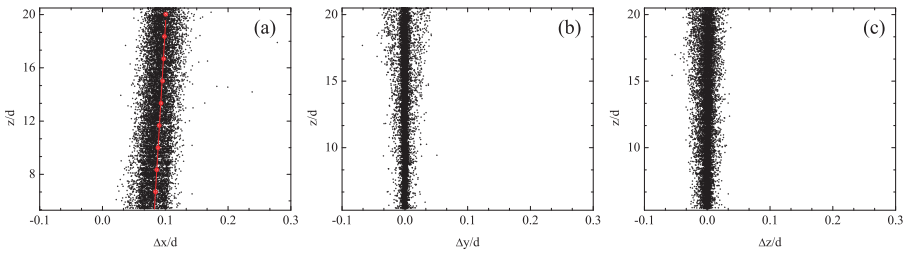

Fig. 3. (Color online) The displacement in (a) flow (x), (b) vorticity (y), and (c) gradient (z) direction as a function z after a strain step imposed by rotating the cell side walls by $2\Delta\theta_0$. The average displacement as a function of height and a linear fit is also shown in (a).

Examining the points in Fig. 3 more closely, it can be noted that the scatter increases as a function of height z inside the cell. This occurs because only the top boundary is allowed to move to accommodate any change in the volume packing of spheres inside the shear cell. Therefore, fluctuations cumulate as a function of height and any changes near the bottom wall necessarily affect the packing of particles near the top of the cell, but not the other way around.

3.2. *Particle displacement distributions*

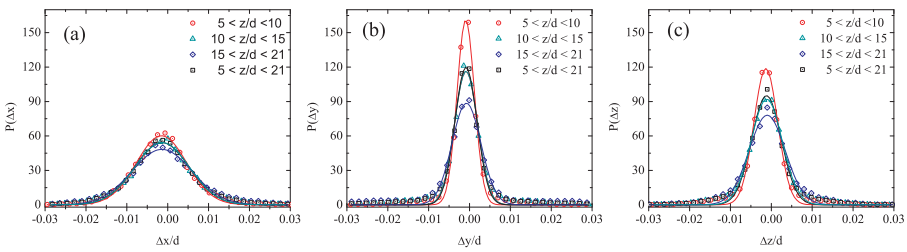

Fig. 4. The distributions of the particle displacement subtracted from the mean displacement corresponding to that height in the (a) flow, (b) vorticity, and (c) gradient directions for $N = 1$ shows fluctuations are anisotropic. Displacement correspond to rotating the side walls through $\Delta\theta_0$. A systematic variation with z can be noted, but the fluctuations averaged over the bulk shear zone imaged coincides with the central z region.

To further analyze the observed raw displacements (Δx_1, Δy_1, Δz_1) shown in Fig. 3, we first obtain the non-affine displacement of the particle by subtracting away the mean displacement due to the applied shear at that height from the measured raw displacement i.e. $\Delta x = \Delta x_1 - \langle \Delta x_1(z) \rangle$, $\langle .. \rangle$ indicates averaging displacements over particles sheared at height z. We then plot the distribution of the non-affine displacement distribution Δx, Δy, and Δz in Fig. 4 in the flow, vorticity, and shear direction for the entire height inside the viewing window, and for windows corre-

sponding to the top, middle, and lower 1/3rd of the window to understand the effect of systematic fluctuations with height. Systematic deviations are noted with z as was qualitatively noted from Fig. 3. However, the distribution plotted over the entire bulk shear zone coincide with the central window, and therefore to improve statistics, we present quantities averaged for $5 < z/d < 21$ as representative of the center of the cell.

It may be noted that the displacement distributions in each direction may be approximately described by a Gaussian. The Gaussian nature of the distributions improves even further if a large wall rotational displacements is used to calculate the distributions. Thus we observe that particles show random fluctuations about their mean positions even though the packing as a whole is sheared uniformly in the x direction. Noting the small magnitudes of the fluctuations relative to the mean strain and the particle, confirms the fact that these are rather high Peclet number flows with diffusion smaller than advection. Now, further examining the width of the distributions, it is clear that the fluctuations are anisotropic with greater fluctuations in the flow direction than the gradient direction, which in turn is greater than the vorticity direction.

3.3. *Mean square displacements*

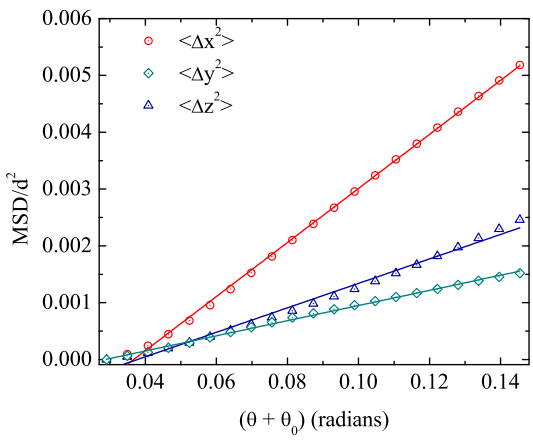

Fig. 5. (Color online) The shear induced particles mean square displacements (MSD) are anisotropic within a shear cycle with greatest growth observed along the flow direction, and least in the vorticity direction. The evolution of non-affine displacements corresponding to half a cycle are shown. The slopes s_i, for $i = x, y, z$ are $s_x = 0.0476 \pm 0.0004$, $s_y = 0.0133 \pm 0.0001$, $s_z = 0.0215 \pm 0.0005$.

To analyze the trends in the particle fluctuations over various applied strain and shear cycles, we examine the mean square displacement which corresponds to the width of the non-affine particle displacement distribution. Because the distributions are described by a Gaussian, the width give a sufficient description of the full distribution. In Fig. 5, we plot in the non-affine mean square displacements (MSD) $\langle \Delta x^2 \rangle$, $\langle \Delta y^2 \rangle$, and $\langle \Delta z^2 \rangle$ as a function of rotation angle of the side walls for cycle number $N = 1$. We use the rotation angle rather than time to plot the MSD be-

cause of the quasi-static nature of the application of strain, therefore fluctuations should scale with applied strain and not strain rate for these systems where particles do not move unless actively pushed. We find that the growth of MSD is clearly anisotropic relative to applied strain, with the fluctuations in the gradient directions less than the flow direction, but lower than the vorticity direction consistent with the anisotropy in the particle displacement distributions. While, in principle one can fit a line through the points (as shown), it is unclear if the observed linearity is over sufficient enough strains to state that the slope corresponds to the components of the long time self-diffusion tensor. However, it may be noted that the observed hierarchy of slopes is consistent with particle self-diffusion observed under shear in simulations on dense suspensions by Foss and Brady.[5] Because the integral of the velocity auto-correlation function gives the diffusion coefficient, the observed anisotropy in the slope of MSD, is also consistent with the overall anisotropic decay of VACF derived by Otsuki and Hayakawa[13] for dilute nearly elastic sheared granular case, and Kumaran[12] for dense granular liquids. MSD obtained over a significantly longer strain can only allow us to test the two theoretical results further, and is the subject of further experiments.

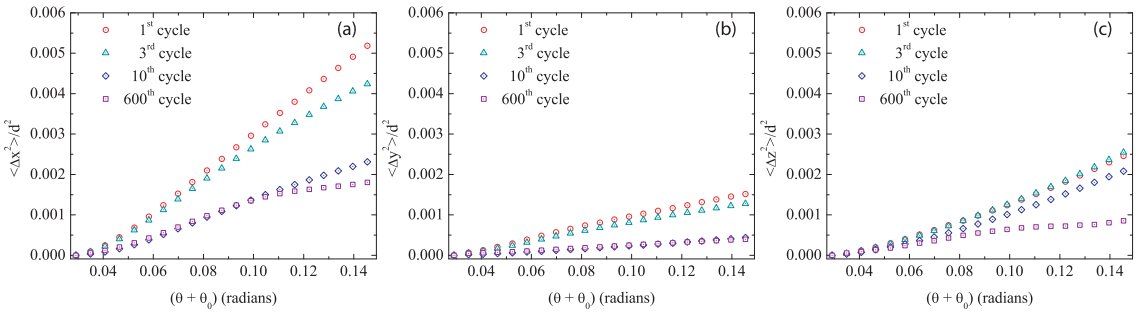

Fig. 6. (Color online) The anisotropic growth of the mean square displacements (MSD) of the particles within a cycle as a function of cycle number. The growth slows down as the system compacts, showing a slow evolution towards arrest.

To understand the response of the system when sheared longer, we have also plotted the MSD for various cycles from $N = 1$ to $N = 600$ in Fig. 6. MSD is observed to grow more slowly for higher N showing that the particle fluctuations get increasingly smaller as the system is sheared and compressed. Further, as can be noted from Fig. 6, the MSD start to display saturation behavior at higher N appearing caged. This must occur because of the particles get more densely packed as the system is sheared. It is interesting to note that the effect of compaction on fluctuations is rather large. MSD is observed to drop by a factor half even though the increase in volume fraction is rather small (see Fig. 2), corresponding to less than 3% increase in ϕ.

To further illustrate that particles essentially compact nearly in the same place and do not diffusive significantly over the scale of a particle diameter, we have plotted the cumulative MSD over the first 150 cycles in Fig. 7, where we have subtracted the small mean drift in the z-direction because of particles settling due to compaction.

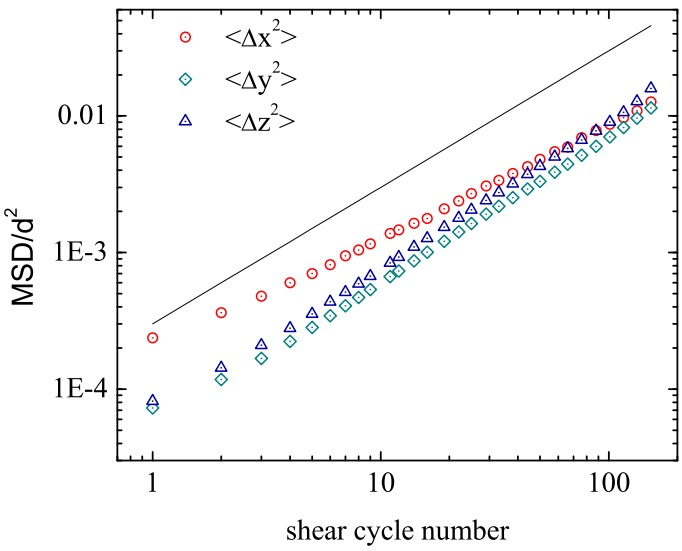

Fig. 7. (Color online) MSD as a function of shear cycle number appear increase homogeneously within experimental error. Further, the overall fluctuations are small compared with the particle size. A line with unit slope is added to guide the eye.

The data as a function of cycle number shows linear growth, but the overall fluctuations are small compared with the particle size. Thus if there is any changes of neighbors, it appears it occurs with cooperation of many particles at least over the initial hundreds of cycles where in fact most of the fast consolidation of the packing has taken place. Our data appears to show that particles essentially settle in place by rearranging relative to neighboring particles, and no fast or large cage breaking of the scale of particle diameter occurs at least over the shear cycles tested at these volume fractions approaching random close packing. Further, the growth of MSD is observed to become fairly homogeneous with increasing shear cycles and no significant signature of the anisotropy observed during positive strain cycle is found for larger N. Thus over a shear cycle, it appears that the sensitivity of fluctuations to the direction over which shear is applied is lost. Most interestingly, the growth of fluctuation in Fig. 7 over several cycles is much smaller than implied by examining only inside positive half of a shear cycle as in Figs. 5, and 6.

We hypothesize that granular fluctuations in fact have a reversible and plastic irreversible response to the application of a perturbative strain *even when particles may be sliding with friction* relative to each other. The plastic response causes the particles to rearrange as a function of cycle number but this response is small compared to the growth observed within a cycle. Therefore it appears that part of the non-affine fluctuations introduced in the positive half of a shear cycle is returned during the negative half of the shear cycle, provided the applied cycle amplitude is small enough. We note that this reversible component is different than simply due to deformation due to elasticity of glass material itself which is immeasurably small because of its high rigidity.

§4. Summary

In summary, we have introduced a cyclic shear apparatus where we measure the three dimensional position of the particles as a function of shear cycle number. Inside a shear cycle, the direction of applied strain is clearly visible in analysis of particle fluctuations. Examining the growth of the over cycle numbers however, gives a different picture, with essentially homogeneous growth of fluctuations. We further find that particle fluctuations decreases significantly as the volume fraction is increases only slightly above the initial packing of 0.59, and the packing evolves towards arrest. Understanding the plastic growth of fluctuations averaged over a range of cycle parameters and relating it to structural rearrangements using cross-correlation functions and free volume distributions is the topic of current work and will be published elsewhere.[20)]

We thank Ashish Orpe and Michael Berhanu for helpful advise on the experiments, and V. Kumaran for many informative conversations on self-diffusion in sheared flows, and Hisao Hayakawa for stimulating discussions. This work was funded by National Science Foundation under CBET-0853943, and was informed by interactions with participants at the 2009 Frontiers of Nonequilibrium Physics Workshop hosted by YKIS.

References

1) J. T. Jenkins and M. W. Richman, Arch. Rat. Mech. Anal. **87** (1985), 355.
2) C. K. K. Lun, S. B. Savage, D. J. Jeffrey and N. Chepurniy, J. Fluid Mech. **140** (1984), 223.
3) I. Goldhirsch, Annual Review of Fluid Mechanics **35** (2003), 293.
4) C.S. Campbell, Journal of Fluid Mechanics **348** (1997), 85.
5) D.R. Foss and J.F. Brady, Journal of Fluid Mechanics **401** (1999) 243.
6) V. Kumaran, Journal of Fluid Mechanics **632** (2009), 109.
7) B. Utter and R. P. Behringer, Phys. Rev. E **69** (2004), 031308.
8) J. Choi, A. Kudrolli, R. R. Rosales, and M. Z. Bazant, Phys. Rev. Lett. **92** (2004), 174301.
9) A. V. Orpe, V. Kumaran, K. A. Reddy and A. Kudrolli, Europhys. Lett. **84** (2008), 64003.
10) A. V. Orpe and A. Kudrolli, Phys. Rev. Lett. **98** (2007), 238001.
11) O. Pouliquen, M. Belzons, and M. Nicolas, Phys. Rev. Lett. **91** (2003), 014301.
12) V. Kumaran, Phys. Rev. E **79** (2009), 011301.
13) M. Otsuki and H. Hayakawa, J. Stat. Mech. (2009), L08003.
14) M. Toiya, J. Stambaugh, and W. Losert, Phys. Rev. Lett. **93** (2004), 088001.
15) J.-C. Tsai, G.A. Voth, and J.P. Gollub, Phys. Rev. Lett. **91** (2003), 064301.
16) S. Siavoshi, A.V. Orpe, and A. Kudrolli, Phys. Rev. E **73** (2006), 010301.
17) C. Rycroft, A.V. Orpe, and A. Kudrolli, Phys. Rev. E **80** (2009), 031305.
18) R. R Hartley and R.P. Behringer, Nature **421** (2003), 928.
19) IDL computing environment, http://www.ittvis.com/
20) A. Panaitescu and A. Kudrolli, unpublished.